Mergers drive spin swings along the cosmic web.

C. Welker, J. Devriendt, Y. Dubois, C. Pichon, S. Peirani

Mergers drive spin swings along the cosmic web

C. Welker,[1,2]★ J. Devriendt,[2] Y. Dubois,[1,2] C. Pichon[1] and S. Peirani[1]

[1]*Institut d'Astrophysique de Paris, UMR 7095, CNRS, UPMC Univ. Paris VI, 98 bis boulevard Arago, F-75014 Paris, France*
[2]*Sub-department of Astrophysics, University of Oxford, Keble Road, Oxford OX1 3RH, UK*

ABSTRACT

The close relationship between mergers and the reorientation of the *spin* for galaxies and their host dark haloes is investigated using a cosmological hydrodynamical simulation (Horizon-AGN). Through a statistical analysis of merger trees, we show that spin swings are mainly driven by mergers along the filamentary structure of the cosmic web, and that these events account for the preferred perpendicular orientation of massive galaxies with respect to their nearest filament. By contrast, low-mass galaxies ($M_s < 10^{10}\,\mathrm{M_\odot}$ at redshift 1.5) having undergone very few mergers, if at all, tend to possess a spin well aligned with their filament. Haloes follow the same trend as galaxies but display a greater sensitivity to smooth anisotropic accretion. The relative effect of mergers on magnitude is qualitatively different for minor and major mergers: mergers (and diffuse accretion) generally increase the magnitude of the specific angular momentum, but major mergers also give rise to a population of objects with less specific angular momentum left. Without mergers, secular accretion builds up the specific angular momentum of galaxies but not that of haloes. It also (re)aligns galaxies with their filament.

Key words: methods: numerical – galaxies: formation – galaxies: haloes – galaxies: kinematics and dynamics – large-scale structure of Universe.

1 INTRODUCTION

Over the past 10 years, several numerical investigations (e.g. Aragón-Calvo et al. 2007; Hahn et al. 2007; Paz, Stasyszyn & Padilla 2008; Sousbie et al. 2008) have reported that large-scale structures, i.e. cosmic filaments and sheets, influence the direction of the intrinsic angular momentum (AM) – or *spin* – of haloes, in a way originally predicted by Lee & Pen (2000). It has been speculated that massive haloes have AM perpendicular to the filament and higher spin parameters because they are the results of major mergers (Aubert, Pichon & Colombi 2004; Peirani, Mohayaee & de Freitas Pacheco 2004; Bailin & Steinmetz 2005). On the other hand, low-mass haloes acquire most of their mass through smooth accretion, which explains why their AM is preferentially parallel to their closest large-scale filament (Codis et al. 2012; Laigle et al. 2013). Using the cosmological hydrodynamical Horizon-AGN simulation, Dubois et al. (2014) have shown that this trend extends to galaxies: the AM of low-mass, rotation-dominated, blue, star-forming galaxies is preferentially aligned with their filaments, whereas high-mass, velocity dispersion-supported, red quiescent galaxies tend to possess an AM perpendicular to these filaments. These theoretical predictions have recently received their first observational support (Tempel & Libeskind 2013). Analysing Sloan Digital Sky Survey data, these authors uncovered a trend for spiral galaxies to align

with nearby structures, as well as a trend for elliptical galaxies to be perpendicular to them.

In this Letter, we revisit these significant findings with an emphasis both on exploring the physical mechanisms which drive halo's and galactic spin swings and on quantifying how much mergers and smooth accretion re-orient these spins relative to cosmic filaments. After a brief review of the numerical methods in Section 2, we analyse the effect of mergers and smooth accretion on AM's orientation and magnitude for haloes and galaxies in Section 3.

2 NUMERICAL METHOD

The cosmological hydrodynamical simulation analysed in this Letter, Horizon-AGN, is already described in Dubois et al. (2014), so we only summarize its main features in this Letter. We adopt a standard Λ cold dark matter cosmology with total matter density $\Omega_m = 0.272$, dark energy density $\Omega_\Lambda = 0.728$, amplitude of the matter power spectrum $\sigma_8 = 0.81$, baryon density $\Omega_b = 0.045$, Hubble constant $H_0 = 70.4\,\mathrm{km\,s^{-1}\,Mpc^{-1}}$, and $n_s = 0.967$ compatible with the *Wilkinson Microwave Anisotropy Probe*-7 data (Komatsu 2011). The size of the simulated volume is $L_{box} = 100\,h^{-1}$ Mpc on a side, and it contains 1024^3 dark matter (DM) particles, which results in a DM mass resolution of $M_{DM,res} = 8 \times 10^7\,\mathrm{M_\odot}$. The simulation is run with the RAMSES code (Teyssier 2002), and the initially uniform grid is adaptively refined down to $\Delta x = 1$ proper kpc at all times. Refinement is triggered in a quasi-Lagrangian manner: if the number of DM particles becomes greater than 8, or the total

★ E-mail: welker@iap.fr

baryonic mass reaches eight times the initial DM mass resolution in a cell. Gas can radiatively cool down to 10^4 K through H and He collisions with a contribution from metals using rates tabulated by Sutherland & Dopita (1993). Heating from a uniform UV background takes place after redshift $z_{reion} = 10$ following Haardt & Madau (1996). The star formation process is modelled using a Schmidt law: $\dot{\rho}_* = \epsilon_* \rho / t_{ff}$ for gas number density above $n_0 = 0.1 \, H \, cm^{-3}$, where $\dot{\rho}_*$ is the star formation rate density, $\epsilon_* = 0.02$ the constant star formation efficiency, and t_{ff} the local free-fall time of the gas. Feedback from stellar winds, and Type Ia and II supernovae is also taken into account for mass, energy, and metal release. Black hole (BH) formation is also included, and they accrete gas at a Bondi-capped-at-Eddington rate and coalesce when they form a tight enough binary. BHs release energy in a quasar (heating) or radio (jet) mode when the accretion rate is above (below) 1 per cent of Eddington, with efficiencies tuned to match the BH–galaxy scaling relations (see Dubois et al. 2012 for details).

Galaxies and haloes are identified with the AdaptaHOP finder (Aubert et al. 2004) which operates on the distribution of star and DM particles, respectively, with the same parameters as in Dubois et al. (2014). Unless specified otherwise, only structures with a minimum of $N_{min} = 100$ particles are considered, which typically selects objects with masses larger than $2 \times 10^8 \, M_\odot$ for galaxies and $8 \times 10^9 \, M_\odot$ for DM haloes. Catalogues containing up to ∼150 000 galaxies and ∼300 000 DM haloes are produced for each redshift output analysed in this Letter ($1.2 < z < 3.8$). Note that, although sub-structures may remain, they are sub-dominant in our sample. The AM – or spin – of a galaxy (halo) is defined as the total AM of the star (DM) particles it contains and is measured with respect to the densest of these star (DM) particles (centre of the structure): $L_s = \Sigma_i m_i (r_i - r_{cm}) \times (v_i - v_{cm})$, with r_i, m_i, and v_i the position, mass, and velocity of particle i, and centre of mass cm. Similarly, we define the specific angular momentum (sAM) of the structure as $l_s = L_s / M_s$, with M_s the total mass of the structure.

The galaxy (halo) catalogues are then used as an input to build merger trees with TreeMaker (Tweed et al. 2009). Any galaxy (halo) at redshift z_n is connected to its progenitors at redshift z_{n-1} and its child at redshift z_{n+1}. We build merger trees for 18 outputs from $z = 1.2$ to 3.8 equally spaced in redshift. On average, the redshift difference between outputs corresponds to a time difference of 200 Myr (range between 100 and 300 Myr). We reconstruct the merger history of each galaxy (halo) starting from the lowest redshift z and identifying the most massive progenitor at each time step as *the galaxy* or *main progenitor*, and the other progenitors as *satellites*. Moreover, we double check that the mass of any child contains at least half the mass of its main progenitor to prevent misidentifications. Note that the definition of mergers (versus smooth accretion) depends on the threshold used to identify objects as any object composed of fewer particles is discarded and considered as smooth accretion. Finally, in order to get rid of objects too contaminated by grid-locking effects (grid/spin alignment trend for the smallest structures; see Dubois et al. 2014), we exclude galaxies with $M_s < 10^9 \, M_\odot$ and haloes with $M_h < 10^{11} \, M_\odot$ from our *main progenitor* sample for spin analysis. Satellites, however, can be smaller structures, which is why we adopt a low object identification mass threshold, and select more massive *main progenitors* afterwards. This two-step procedure allows for a clear separation of main progenitors and satellites and avoids significant signal loss. Note that, in all figures where haloes and galaxies are compared, the ratio of main progenitor minimal mass to satellite minimal mass is the same, so as to permit a fair comparison between both categories of objects.

In order to quantify the orientation of galaxies (haloes) relative to the cosmic web, we use a geometric three-dimensional ridge extractor called the 'skeleton' (Sousbie, Colombi & Pichon 2009) computed from a density cube of 512^3 cells drawn from the simulation and Gaussian-smoothed with a smoothing length of $3 \, h^{-1}$ Mpc comoving. The orientation of the spin of galaxies (haloes) can then be measured relative to the direction of the closest filament segment.

3 SPIN SWINGS AND MERGERS

First, we define $\delta m = \Delta m_{mer}(z_n) / M(z_n)$ as the mass fraction of an object that is accreted via mergers. In this expression, $M(z_n)$ is the total stellar (DM) mass of a galaxy (halo) at redshift z_n and $\Delta m_{mer}(z_n)$ is the stellar (DM) mass accreted by this galaxy (halo) through mergers between redshifts z_{n-1} and z_n. In a similar spirit, we also define the relative sAM variation of an object between simulation outputs $n - p$ and n as $\delta\lambda_p = (l_{n+p-1} - l_{n-1})/(l_{n+p-1} + l_{n-1})$, where l_n is the magnitude of the object sAM at redshift z_n.

Fig. 1 (top panel) displays the probability distribution function (PDF) of $\cos \Delta\alpha$, where $\Delta\alpha$ is the variation in the angle of the galaxy's AM between time outputs $n - 1$ and $n + 1$, for galaxies
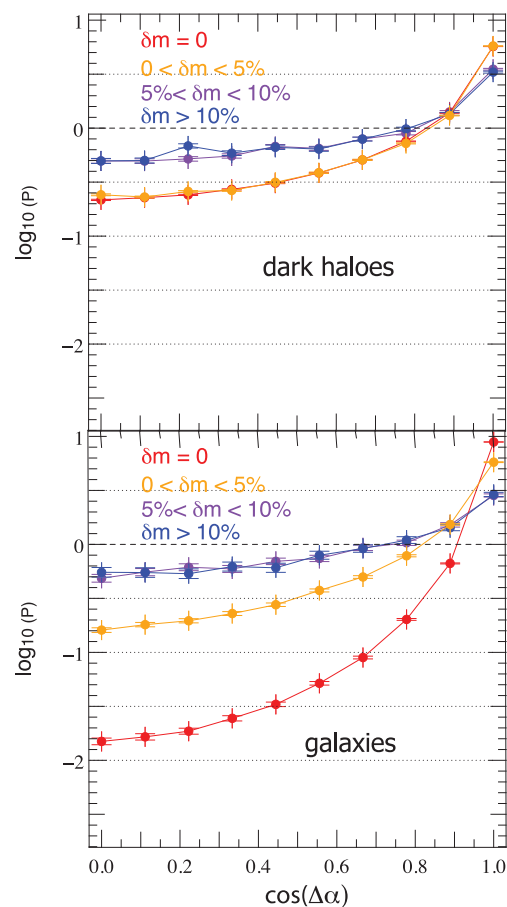

Figure 1. Logarithm of the PDF of $\cos \Delta\alpha$, the cosine of the spin swing angle for galaxies (top panel) and haloes (bottom panel) between time steps $n - 1$ and $n + 1$, for objects with different merger histories. The dashed line corresponds to the uniform PDF, i.e. no preferred orientation. The dotted lines show the threshold below which the population in the bin is 30, 10, 3, and 1 per cent of the sample considered. δm is the mass fraction accreted through mergers between two consecutive time outputs. $\delta m = 0$ corresponds to the no-merger case, i.e. pure smooth accretion. Mergers are responsible for spin swings; haloes are more sensitive to smooth accretion.

with different merger histories, i.e. different values of δm. We recall that the satellite detection threshold is set at $N_{min} = 100$ particles, but that only main progenitors with masses $M_s > 10^9\,M_\odot$ (galaxies) and $M_h > 10^{11}\,M_\odot$ (haloes) are considered. From this figure, one can see that mergers are clearly the main drivers for galaxy spin swings, while the spins of galaxies without mergers tend to remain aligned between time outputs. Indeed, 91 per cent of the latter see their spin stay within an angle of 25 deg over two time outputs (each separated by $\Delta z = 0.1$) whereas this happens only for 28 per cent of galaxies with a merger mass fraction above 5 per cent (this ratio even falls down to 10 per cent with $N_{min} = 1000$). Such a swing effect is sensitive to the merger mass fraction and, as one would expect, tends to be stronger for larger fractions. For $\delta m > 5$ per cent, 50 per cent of the galaxy sample underwent a spin swing >45 deg while this is true for only 18 per cent of galaxies with $0 < \delta m < 5$ per cent and less than 2.5 per cent of the no-merger ($\delta m = 0$) population. However, even mergers with low mass ratio (i.e. mergers where the satellite is less than 20 times lighter than the main progenitor) trigger important swings compared to the no-merger case. Only 58 per cent of the galaxies which underwent a minor merger ($0 < \delta m < 5$ per cent) maintain a spin within a cone of 25 deg over two time outputs (compared to 91 per cent for non-mergers). This behaviour is consistent with the well-known fact that when two galaxies merge, the remnant galaxy acquires a significant fraction of AM through the conversion of the orbital AM of the pair rather than simply inheriting the AM of its progenitors.

A similar analysis for DM haloes confirms that they qualitatively follow the same behaviour as galaxies but with quantitative variations due to the fact they are velocity dispersion-supported structures rather than rotationally supported ones. More specifically, one can see from Fig. 1 that unlike galaxies, even haloes defined as non-mergers ($\delta m = 0$) exhibit noticeable spin swings (see also Bett & Frenk 2012). This can be attributed to the net AM of haloes resulting from random motions of DM particles (by opposition to ordered rotational motion of star particles for galaxies): even a small amount of AM brought in coherently by smooth accretion or mergers will be enough to noticeably influence the direction of the halo spin vector. Note that large-scale tidal torques also apply more efficiently to haloes than galaxies due to the larger spatial extent of the former, and we speculate that these torques could also contribute to some of the quantitative differences we measure between AM alignment of haloes and galaxies. Given that mergers account for the spin swings of galaxies, they should also be responsible for setting the orientation of their spins relative to the filament, at least for massive galaxies which do experience a significant amount of mergers. Our results are consistent with this scenario, as can be seen in Fig. 2 where we plot the PDF of μ, the cosine of the angle between the galactic AM and the direction of its filament, ξ being the excess probability with respect to a uniform distribution. It demonstrates that galaxies (each one being counted once after each merger) which have just merged tend to show a spin more perpendicular to filaments, and that the signal is stronger for galaxies which have experienced a larger number of mergers during their lifetime (from redshift of birth to the redshift of measurement). This is a strong argument in favour of orbital AM transfer into spin since mergers are preferentially the result of galaxy encounters along cosmic filaments, i.e. pairs with an orbital AM that is orthogonal to the filament. Note that the excess probability $\xi \simeq 0.1$–0.2 of being perpendicular to their filament for galaxies undergoing mergers is larger than when the same galaxies are simply split into sub-samples according to their physical properties: mass, colour, activity, etc. ($\xi < 0.05$ in that case; see Dubois et al. 2014).
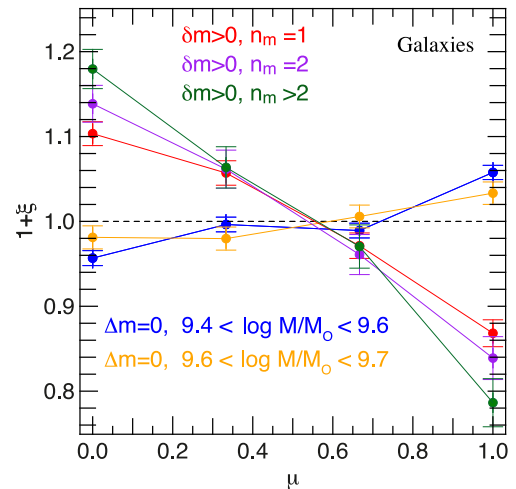

Figure 2. PDF of μ, the cosine of the angle between the galactic spin and its filament for different galaxy merger histories. This plot shows cumulative results for all simulation galaxies identified between $z = 3.16$ and 1.71. ξ is the excess probability with respect to a uniform distribution (dashed line). As before, δm is the fraction of mass accreted through mergers between two consecutive time outputs and n_m is the total number of mergers a galaxy has undergone at the time of the measurement. $\Delta m = 0$, with Δm the cumulative merger fraction corresponds to the absence of mergers over the lifetime of the galaxy. The stronger the merger rate, the stronger the misalignment. Subsequent mergers amplify the alignment.

In contrast, spins of galaxies with no merger are more likely to be aligned with their filament. Note that the threshold for structure detection here was set to $N_{min} = 1000$ particles, which implies that 'merger' galaxies are more clearly identified than 'non-merger' ones in this figure. The alignment signal is therefore weaker, as expected. To emphasize this selection effect, the excess probability of alignment was analysed for galaxies split into different mass bins, the lowest two of which we plot in Fig. 2. Comparing both measurements, there is indeed tentative evidence that the excess probability of alignment is weaker for higher mass galaxies, which are more likely to have accreted 'undetected' mergers. Note that the alignment signal is completely lost when we consider that sub-sample of galaxies with masses above $10^{10}\,M_\odot$. Further analysis confirms that lower thresholds ($N_{min} < 1000$) attenuate the orthogonal misalignment and strengthen the alignment excess probabilities.

Turning to the magnitude of the sAM, Fig. 3 shows the PDF of $\delta\lambda_2$ for both galaxies and haloes. We can see from this figure that mergers with mass ratios $5 < \delta m < 10$ per cent tend to increase the magnitude of the object sAM (curves are skewed towards positive $\delta\lambda_2$), and that this effect becomes stronger as the mass ratio increases, up to mass fractions around $\delta m > 10$ per cent for which $\sim$75 per cent of haloes and galaxies see their sAM magnitude increase – by a factor 2 or more for $\sim$25 per cent of haloes and galaxies – between two consecutive time outputs.

This behaviour indicates that most mergers contribute constructively to the sAM of the collapsed structures. This is especially true for halo mergers where it can be understood as the conversion of orbital AM into AM of the massive host. For minor ($\delta m < 5$ per cent) to intermediate ($5 < \delta m < 10$ per cent) galaxy mergers, satellites are most likely progressively stripped of their gas and stars and swallowed in the rotation plane of the central object, therefore increasing the rotational energy. However, major mergers ($\delta m > 10$ per cent) – where an important part of the rotational energy can be converted to random motion energy through violent relaxation, intense star
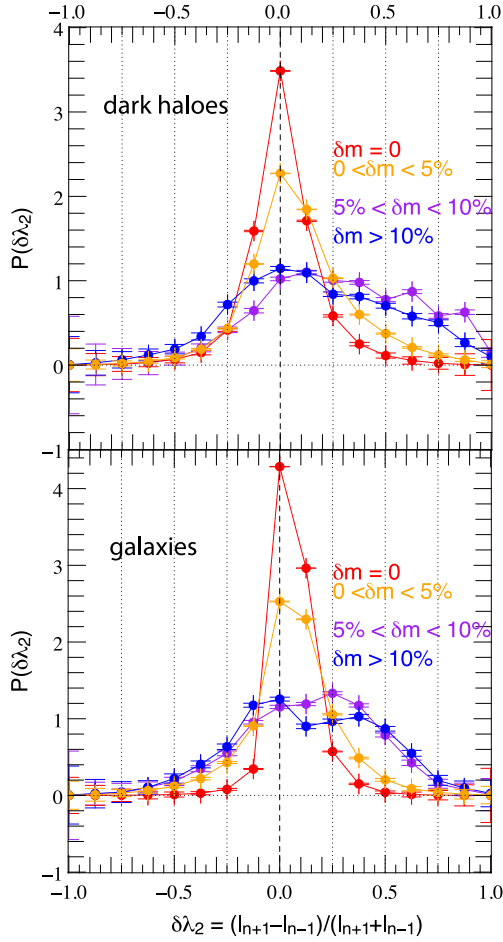
Figure 3. PDF of $\delta\lambda_2$ of the halo's (top panel) and galactic (bottom panel) sAM, for objects with different merger ratios. Positive values correspond to objects which acquire sAM through mergers; negative values correspond to objects which lose sAM. This plot shows results for the entire population of objects identified between $z = 3.8$ and 1.2. Mergers increase the sAM's magnitude.

Figure 4. Same as Fig. 3 for objects which do not merge and for different lookback times. Secular accretion builds up the sAM of galaxies but not that of haloes.

formation and feedback – can in fact contribute destructively to the sAM of the galaxy remnant. Indeed, those mergers induce wings in the PDF of $\delta\lambda_2$ corresponding to galaxies with increasing and decreasing sAM.

With $\delta m = 0$, the PDF bends towards positive $\delta\lambda_2$, suggesting that smooth gas accretion on galaxies, unlike smooth DM accretion on haloes, tends to increase their sAM over time. In order to probe this (re)alignment process further, we present in Fig. 4 the evolution of the PDF of $\delta\lambda_{p-n} \equiv (l_p - l_n)/(l_p + l_n)$, where l_p is the sAM magnitude at redshift z_p and $p = n + 1, n + 2, n + 3$ indicates different lookback time outputs, for haloes and galaxies. It appears clearly that while the halo distribution remains symmetric over time, the galaxy distribution shifts towards positive values with an average peak drift time-scale of $t_{\delta\lambda} \simeq 5-10$ Gyr. We measure a similar trend for different galaxy mass bins up to $M_s = 10^{11}$ M$_\odot$ (albeit with a slower drift for the most massive galaxies with $M_s \approx 10^{11}$ M$_\odot$).

These findings favour the idea that cold gas (either cold streams or diffuse cooling gas) spins up galaxies over time. This secular gas accretion on to galaxies also (re)aligns the galaxy with its filament. This is demonstrated in Fig. 5, which is obtained via stacking for four successive time steps the relative orientation of the spins of galaxies to filaments when no merger occurs. It shows that the excess
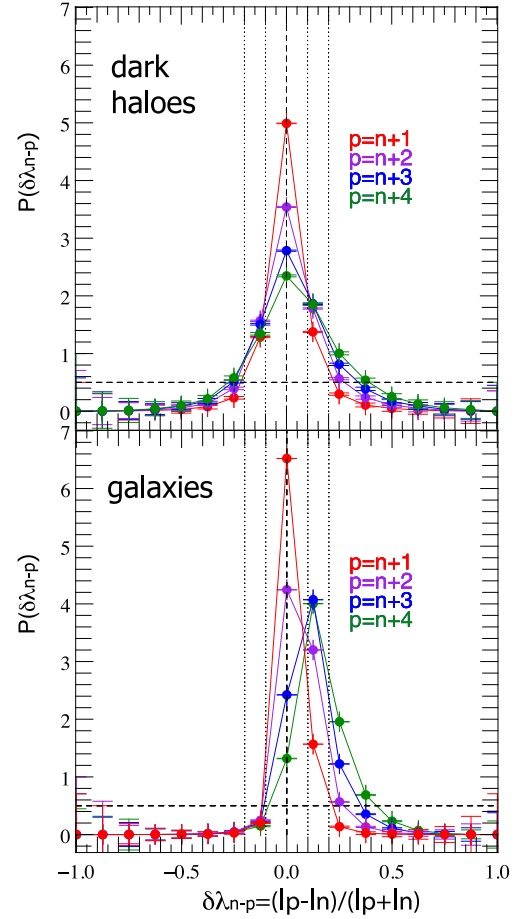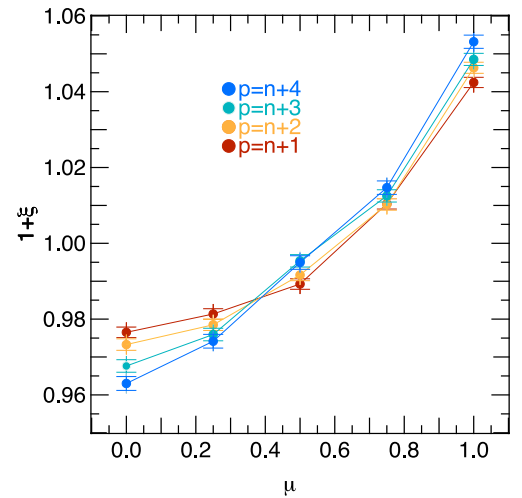

Figure 5. Same as Fig. 2 for galaxies which do not merge and for different lookback times (but samples of comparable size). In the absence of merger, galaxies tend to realign with their filament over time.

probability of alignment is amplified with time in the absence of mergers.

To sum up, Tempel & Libeskind (2013) found that spiral galaxies tend to have a spin aligned to their nearest filament while the spin of S0 galaxies is more likely to show an orthogonal orientation. Dubois et al. (2014) argue that a transition mass can be associated with this change in spin orientation, which is reasonably bracketed between $\log(M_s/M_\odot) = 10.25$ and 10.75. These authors also point out that such a mass loosely corresponds to the characteristic mass at which a halo extent becomes comparable to that of the vorticity quadrant in which it is embedded within its host filament (Laigle et al. 2013). Such a mass-dependent scenario was first suggested by Hahn et al. (2007) and quantified by Codis et al. (2012) for DM haloes. The key idea which underpins all these studies is that lighter galaxies acquire most of their spin through secondary infall from their (aligned with the filament) vorticity-rich environment, while more massive galaxies acquire a large fraction of theirs via orbital momentum transfer during merger events which mainly take place along the direction of the large-scale filament closest to them. This Letter showed that galaxies without merger both realign to their host filament and increase their sAM, while successive mergers drive the remnant's spin perpendicular to it, and depending on the strength of the merger, decrease or redistribute the remnant's sAM magnitude. Hence, it strongly favours the idea that cold/cooling flows feed low-mass disc galaxies [with anisotropic gas streams along the vorticity-rich filaments, as advocated in Pichon et al. (2011), or possibly through smooth gas accretion from the spinning host haloes], therefore enhancing their sAM magnitude over time. It also demonstrates that mergers are responsible for the spin swings as suggested by previous investigations.

4 CONCLUSION

Using the Horizon-AGN cosmological gas dynamics simulation, we have analysed the variations of AM orientation and magnitude of galaxies and haloes as a function of their merger rates. Our statistical analysis of merger trees shows that spin swings are driven by mergers, which have a strong impact on both the *orientation* and the *magnitude* of the AM. Our findings are the following.

(i) The stronger the strength of the merger, the larger the memory loss of the post-merger spin direction of dark haloes and galaxies.

(ii) The alignment of the spin of an object with the cosmic web depends on its merger history: the more mergers contribute to its mass, the more likely its spin will be perpendicular to its filament.

(iii) When the merger contribution to the mass of an object is negligible (<1 per cent), the modulus of the sAM of *galaxies* still increases with time via smooth accretion. Moreover, the orientation of these spins drift towards (re)alignment with the filament; this does not happen to the sAM of DM haloes, whose magnitude remains independent of time on average.

(iv) Mergers (with mass ratios >10 per cent), like smooth accretion, also tend to build up the sAM modulus but of both haloes and galaxies in this case; on the other hand, they also produce a low-sAM tail in the magnitude distribution.

REFERENCES

Aragón-Calvo M. A., van de Weygaert R., Jones B. J. T., van der Hulst J. M., 2007, ApJ, 655, L5
Aubert D., Pichon C., Colombi S., 2004, MNRAS, 352, 376
Bailin J., Steinmetz M., 2005, ApJ, 627, 647
Bett P. E., Frenk C. S., 2012, MNRAS, 420, 3324
Codis S., Pichon C., Devriendt J., Slyz A., Pogosyan D., Dubois Y., Sousbie T., 2012, MNRAS, 427, 3320
Dubois Y., Devriendt J., Slyz A., Teyssier R., 2012, MNRAS, 420, 2662
Dubois Y. et al., 2014, MNRAS, in press
Haardt F., Madau P., 1996, ApJ, 461, 20
Hahn O., Carollo C. M., Porciani C., Dekel A., 2007, MNRAS, 381, 41
Komatsu E. et al., 2011, ApJS, 192, 18
Laigle C. et al., 2013, preprint (arXiv:1310.3801)
Lee J., Pen U., 2000, ApJ, 532, L5
Paz D. J., Stasyszyn F., Padilla N. D., 2008, MNRAS, 389, 1127
Pichon C., Pogosyan D., Kimm T., Slyz A., Devriendt J., Dubois Y., 2011, MNRAS, 418, 2493
Sousbie T., Pichon C., Colombi S., Pogosyan D., 2008, MNRAS, 383, 1655
Sousbie T., Colombi S., Pichon C., 2009, MNRAS, 393, 457
Sutherland R. S., Dopita M. A., 1993, ApJS, 88, 253
Tempel E., Libeskind N. I., 2013, ApJ, 775, L42
Teyssier R., 2002, A&A, 385, 337
Tweed D., Devriendt J., Blaizot J., Colombi S., Slyz A., 2009, A&A, 506, 647

This paper has been typeset from a T_EX/L^AT_EX file prepared by the author.